NANOSYSTEMS: PHYSICS, CHEMISTRY, MATHEMATICS, 2017, 8 (3), P. 397–405

Cryometry data and excess thermodynamic functions in the binary system: water soluble bis-adduct of light fullerene C_{70} with lysine. Assymmetrical thermodynamic model of virtual gibbs energy decomposition – VD-AS

N. A. Charykov[1,5], K. N. Semenov[2], V. V. Keskinov[1], P. V. Garamova[1], D. P. Tyurin[1], I. V. Semenyuk[1], V. V. Petrenko[1], A. V. Kurilenko[1], M. Yu. Matuzenko[1], N. A. Kulenova[3], A. A. Zolotarev[1], D. G. Letenko[4]

[1]Saint Petersburg State Technological Institute (Technical University), Moskovsky prospect, 26 Saint Petersburg, 190013, Russia

[2]Saint Petersburg State University,7/9 Universitetskaya emb., Saint Petersburg, 199034, Russia

[3]D. Serikbayev East Kazakhstan state technical university, A. K. Protozanov Street, 69, Ust-Kamenogorsk city, 070004, The Republic of Kazakhstan

[4]Saint Petersburg State University of Architecture and Civil Engineering (SPSUACE), 2-nd Krasnoarmeiskaya St. 4, 190005 Saint Petersburg, Russia

[5]Saint Petersburg Electrotechnical University "LETI", ul. Professora Popova 5, 197376 Saint Petersburg, Russia

keskinov@mail.ru

PACS 61.48.+c **DOI 10.17586/2220-8054-2017-8-3-397-405**

The temperature of water-ice crystallization initiation decreases (ΔT) were determined in the binary water solutions of water soluble derivative of light fullerene C_{70} with amino-acid lysine at 272.99 – 273.15 K. Partial molar excess functions for H_2O were calculated. For the thermodynamic description of our systems, we have elaborated an original semi-empirical model VD-AS (Virial Decomposition Asymmetric Model), based on the virial decomposition of the molar Gibbs energy of the component molar fractions in the solution. With the help of the VD-AS model, partial molar functions of nano-clusters were calculated. Excess and full average Gibbs energies for the solutions and miscibility gaps concentration regions (with the help of diffusional instability equations) were calculated. Thus, the VD-AS model excellently describes pre-delamination or micro-heterogeneous-structure formation in the considered solutions. These calculations were accordingly confirmed by dynamic light scattering data.

Keywords: cryometry, light fullerene C_{70}, lysine, thermodynamic model.

Received: 15 April 2017

Revised: 14 May 2017

1. Introduction

The article is a continuation of the investigations devoted to the synthesis, identification and investigation of physico-chemical properties of water soluble of light fullerene (C_{60} and C_{70}) derivatives, such as: complex eithers of two-based carbonic acids (malonates, oxalates), poly-hydroxylated forms (fullerenols), amino-acid derivatives (argenine, alanine) some other derivatives [1–23]. In these works, in particular, the physico-chemical properties of aqueous light fullerene derivative solutions, depending on the solutions' concentrations, were investigated: poly-thermal solubility and crystal hydrate compositions; volume properties (density, average and partial component molar volumes); refractive indices, specific and molar refractions; conductivity and pH (apparent dissociation degrees and concentration dissociation constants); associates dimensions and electro-kinetic ξ – potentials, etc.

The investigation of such fullerenes derivatives is necessary for the following reasons:

First: The application of fullerenes considerably limited by their almost complete incompatibility with water and aqueous solutions, such as, for example: physiological solution, blood, lymph, gastric juice etc. Solubility of light fullerenes, for example, in pure water at 25°C is practically negligible (10^{-12}–10^{-14} g/dm^3 for C_{60} and C_{70}, correspondingly).

Second: These fullerene derivatives, with amino-acids possess unique anti-oxidant, antibacterial, antiviral and antifungal properties, can absorb different type free radicals, UV photons etc. These facts determine high potential for its application in medicine, pharmacology, cosmetics, food and wine industry etc.

The investigation of the excess thermodynamic functions in such systems (activities, activity coefficients, excess (or mixing) Gibbs energies (enthalpies, entropies) etc.), to the best of our knowledge, until this time, has not been provided, except for two original works [24, 25]. In those articles, in the binary systems with the help of cryometry investigations, the authors determined the decrease in temperature for ice crystallization initiation

(liquidus temperatures), water activities, water activity coefficients, and then, solving numerically the Gibbs-Duhem equation – activities and activity coefficients of fullerene derivatives. No other data concerning the excess function in the considered systems, obtained, for example by the isopiestic method, have been found. Meanwhile, such data may be very scientifically interesting, because these aqueous solutions have very specific and rare consistent hierarchical type of association (see below).

2. Cryometry data in the binary water solutions of water soluble light fullerene derivatives

The temperature of water-ice crystallization initiation decreases (ΔT) were determined in binary aqueous solutions of water-soluble light fullerene derivative: $C_{70}(C_6H_{13}N_2O_2)_2$ – H_2O at 272.99 – 273.15 K. The temperature range corresponds to concentration range X (Molar fraction of $C_{70}(C_6H_{13}N_2O_2)_2$ in the solution) = 0–$1.38{\cdot}10^{-4}$ rel. un. or C (volume concentration) $\approx$ 0–10 g/dm^3. Such concentrations range for fullerene containing systems is wide enough and corresponds to the solubility of $C_{70}(C_6H_{13}N_2O_2)_2$ in water at 273.15 K. Even at these concentrations, the solutions may lose the diffusive stability, i.e. pre-flake (see below).

Solution concentrations (in molar fractions) vary over a wide range $x_{nano-cluster} = 1.1 \cdot 10^{-6}$ – $1.4 \cdot 10^{-4}$ rel.un. The liquidus temperatures were determined with the help of Beckman thermometer with the linear resolution of the device scale $\Delta T/\Delta h \approx 0.01$ K/mm (h – height of Hg capillary raising). Cryometry data $\Delta T(x_{nano-cluster})$ are shown in Fig. 1 and in Table 1.

TABLE 1. Cryometry data and excess thermodynamic functions for the bis-lysine adduct of C_{70} light fullerene – $C_{70}(C_6H_{13}N_2O_2)_2$ – H_2O binary system at 272.99–273.15 K. Asymmetrical model of excess Gibbs energy decomposition model – VD-AS is used

Molar fraction of $C_{70}(C_6H_{13}N_2O_2)_2$ in the solution $X_{C70(C6H13N2O2)2}$ (rel.un.)	Ice crystallization initiation temperature decrease ΔT (K)	$\ln a_{H2O}$ ln(water activity) (rel.un.)	$\ln \gamma_{H2O}$ ln (water activity coefficient) (rel.un.)	$\ln \gamma^{as}_{C70(C6H13N2O2)2}$ ln (activity coefficient of $C_{70}(C_6H_{13}N_2O_2)_2$ (rel.un.)
0.000	0.000	0.000	0.000	0.000
$1.083{\cdot}10^{-6}$	0.005	$-5.86{\cdot}10^{-5}$	$-5.75{\cdot}10^{-5}$	3.38
$2.166{\cdot}10^{-6}$	0.013	$-1.44{\cdot}10^{-4}$	$-1.42{\cdot}10^{-4}$	6.65
$4.332{\cdot}10^{-6}$	0.020	$-2.22{\cdot}10^{-4}$	$-2.18{\cdot}10^{-4}$	12.9
$8.66{\cdot}10^{-6}$	0.030	$-$-3.33$\cdot 10^{-4}$	$-3.25{\cdot}10^{-4}$	24.3
$1.73{\cdot}10^{-5}$	0.050	$-5.49{\cdot}10^{-4}$	$-5.32{\cdot}10^{-4}$	42.2
$3.46{\cdot}10^{-5}$	0.075	$-8.22{\cdot}10^{-4}$	$-7.87{\cdot}10^{-4}$	66.0
$6.92{\cdot}10^{-5}$	0.11	-0.00122	-0.00116	72.5
$1.38{\cdot}10^{-4}$	0.16	-0.00178	-0.00164	73.1

Expanded uncertainties are: $U(\Delta T) = \pm 0.002$ (dilute solutions) – 0.005 (concentrated solutions) K, $U_r(\ln a_{H_2O}) = 0.5$ (concentrated solutions) – 5 (dilute solutions) rel. %, $U_r(\ln \gamma_{H_2O}) = 0.5$ (concentrated solutions) – 5 (dilute solutions) rel. % and $U_r(\ln \gamma_1^{ass}) = 2$ (dilute solutions) – 5 (concentrated solutions) rel.% (as the sum result of experimental errors and numerical approximation).

One can see, that all dependencies $\Delta T(x_{nano-cluster})$ are sharply nonlinear, which prove very high positive deviations of the solutions from ideality for all solutions, even those which are very dilute. In Fig. 1, for comparison, the arrow represents the value ΔT^{id} for the ideal non-electrolyte solution. We can see the experimental ΔT exceeds ΔT^{id} by 1–2 orders of magnitude (for comparable concentrated and dilute solutions, correspondingly). So, one should expect probably gigantic positive deviations of the solution from the ideality in a thermodynamic sense.

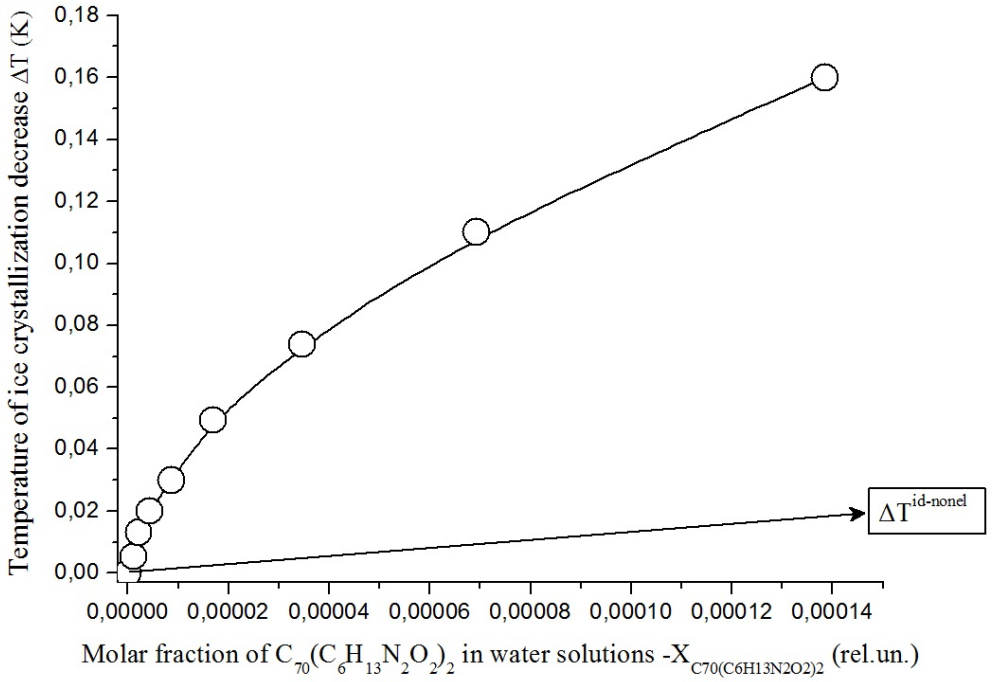

FIG. 1. Temperature of water-ice crystallization beginning (liquidus temperature) decrease (ΔT) against molar fraction concentration in the binary solutions: $C_{70}(C_6H_{13}N_2O_2)_2$ – H_2O at 272.99 – 273.15 K. Arrow shows ΔT-function for the ideal non-electrolyte solution

3. Calculation of water excess functions

For calculating the water activity we have used the well-known equation obtained from the equality of chemical H_2O potentials in pure solid ice and non-ideal liquid solution [34, 35]:

$$\left[-\Delta H_W^f \Delta T - \Delta C_P \Delta T^2\right] / \left[R\left(T_0^f - \Delta T\right) T_0^f\right] = \ln a_{H2O}, \tag{1}$$

where ΔH_W^f = 5990 J/mole, $\Delta C_P = -38.893$ J/mole·K, $T_0^f = 273.15$ K heat, temperature of ice fusion and change of heat capacity in the process of ice fusion, correspondingly. Equation (1) was displayed in the symmetrical normalization scale for thermodynamic functions for both solution components:

$$a_{H2O}(x_{H2O} = 1) = \gamma_{H2O}(x_{H2O} = 1) = 1, \tag{2}$$

$$a_{nano-cluster}\,(x_{nano-cluster} = 1) = \gamma_{nano-cluster}(x_{nano-cluster} = 1) = 1, \tag{3}$$

where x_i and a_i, γ_i – molar fraction, activity and activity coefficient of i-th component.

Calculated data for $\ln[a_{H2O}(x_{nano-cluster})]$ are represented in Fig. 2 and Table. 1.

Additional researchers [24, 25] calculated concentration dependencies $\ln\gamma_{H2O}$, derivatives $d\ln\gamma_{H2O}/dx_{nano-cluster}$ (numerically). Then, other researchers [34, 35] calculated the dependencies $d\ln\gamma_{nano-cluster}/dx_{nano-cluster}$, (according to the classical Gibbs–Duhem differential equation) also numerically and at the end by numerical integration the dependencies $\ln\gamma_{nano-cluster}(x_{nano-cluster})$ were calculated. As a result, as was previously expected, gigantic positive deviations of the solution from ideality for the functions $\ln\gamma_{nano-cluster}$ were obtained $\ln\gamma_{nano-cluster} \approx n(10^0 - 10^1)$ (see Table 1 and Fig. 4). Naturally, in all likelihood, no existing thermodynamic model can describe such nontrivial behavior of nano-cluster thermodynamic functions.

4. Virial Decomposition Asymmetric Model – VD-AS

For the description of such nontrivial thermodynamic behavior of the considered aqueous solutions, we have elaborated semi-empirical model VD-AS (Virial Decomposition Asymmetric Model), based on the virial decomposition of excess molar Gibbs energy on the solution for the components molar fractions. This technique has often been used for the thermodynamic description of binary and multicomponent systems with different physico-chemical nature, such as: electrolyte solutions [26–29], non-electrolyte (semiconductor) melts [30–33], isovalent

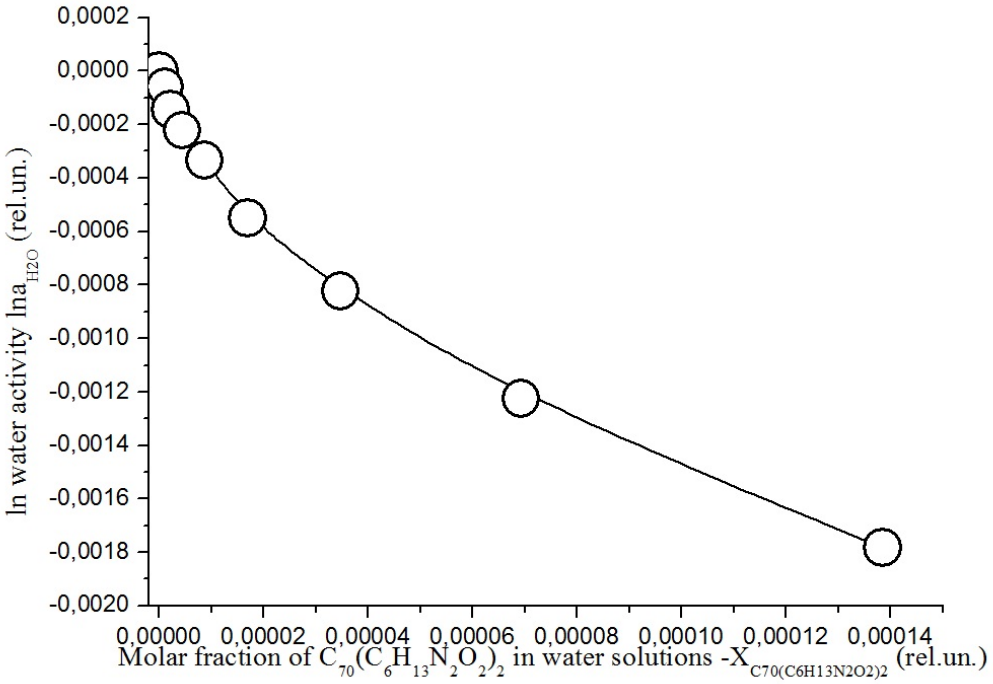

FIG. 2. Logarithm of water activity ($\ln a_{H2O}$) against molar fraction concentration in the binary solutions: $C_{70}(C_6H_{13}N_2O_2)_2$ – H_2O at 272.99 – 273.15 K

substitution solid solutions [34–36]. If one takes only one term in the decomposition for the binary system (corresponding to the invariant second virial coefficient), see later equation (4) well-known strictly regular solutions model – RSM, is realized. Under the assumption of temperature dependence for the only virial coefficient, a quasi-regular solution model – QRSM is realized. If one uses third virial coefficients for the decomposition, a sub-regular solution model – SRSM is realized. Finally, when one alsoconsiders the contribution of the electrostatic non-specific interactions (according to Debye–Huckel theory) Pitzer's model in different variants is realized.

So, we assume the following numeration: 1 – is the number of the dissolved component (nano-cluster in our case), 2 – is the number of the solvent (H_2O). Let us propose the following expression:

$$G^{ex}/RT = (n_1 + n_2) \sum_{i=1} \sum_{j=1} X_1^i X_2^j \cdot \lambda_{ij} = \left(\sum_{i=1} \sum_{j=1} n_1^i n_2^j \cdot \lambda_{ij} \right) / (n_1 + n_2)^{i+j-1}, \tag{4}$$

where G^{ex} – full molar excess solution Gibbs energy, $R = 8.31$ J/K, T – temperature (K), n_i and X_i – molar number and molar fraction of i-th component, correspondingly, λ_{ij} – ij-th virial coefficient in the decomposition of G^{ex}/RT on the component molar numbers. In other words, λ_{ij} are naturally identified as divided by RT specific energy of interaction of i particles of the 1-st component and j particles of the 2-nd component. If one takes into account the huge ($\sim$ two orders of magnitude) differences in the components' molar masses (1-st are heavy) and its linear dimensions (almost one order – nanoclusters, in our case, are hollow), it is quite clear, that if the upper limit of the summation, according to the 1-st component, is a small natural number (not more than 4–6), the upper limit of the summation, according to the 2-nd component, may be more by one-two orders of magnitude.

Let us calculate excess thermodynamic functions of the components: $\ln \gamma_i$:

$$\ln \gamma_1 = \partial \left(G^{ex}/RT \right) / \partial n_1 = \sum_{i=1} \sum_{j=1} \left[i - (i + j - 1) X_1 \right] X_1^{i-1} X_2^j \cdot \lambda_{ij}, \tag{5}$$

$$\ln \gamma_2 = \partial \left(G^{ex}/RT \right) / \partial n_2 = \sum_{i=1} \sum_{j=1} \left[j - (i + j - 1) X_2 \right] X_1^i X_2^{j-1} \cdot \lambda_{ij}. \tag{6}$$

In our case, molar fractions of the components are incomparable:

$$X_2 \gg X_1, \quad X_2 > 0.999 \approx 1, \quad X_1 \ll 1. \tag{7}$$

Thus, equations (5), (6) may be simplified:

$$\ln \gamma_1 \approx \sum_{i=1} i X_1^{i-1} \sum_{j=1} \lambda_{ij}, \tag{8}$$

$$\ln \gamma_2 \approx \sum_{i=1} (1-i) X_1^i \sum_{j=1} \lambda_{ij} = \sum_{i=2} (1-i) X_1^i \sum_{j=1} \lambda_{ij}. \tag{9}$$

From the systems (5), (6) and (8), (9) , one can see that, they agree in a thermodynamic sense, i.e. Gibbs–Duhem equation is valid at T, $P = const$:

$$X_1 d \ln \gamma_1 + X_2 d \ln \gamma_2 = 0, \tag{10}$$

or, for example, from the equations (7), (8) we can get identity:

$$X_1 \sum_{i=1} i (i-1) X_1^{i-2} \lambda_{ij} dX_1 + \sum_{i=1} (1-i) i X_1^{i-1} \lambda_{ij} dX_1 = 0. \tag{11}$$

Let us transfer system (8), (9), denoting as Λ_i summary virial coefficients:

$$\sum_{j=1} \lambda_{ij} = \Lambda_i (T), \tag{12}$$

so, in our conditions of consideration:

$$\ln \gamma_1 \approx \sum_{i=1} i \Lambda_i X_1^{i-1}, \tag{13}$$

$$\ln \gamma_2 \approx \sum_{i=1} (1-i) \Lambda_i X_1^i = \sum_{i=2} (1-i) \Lambda_i X_1^i. \tag{14}$$

One can see that if $\Lambda_1 \neq 0$, then logarithms of the limit activity coefficients – $\ln \gamma_i^0 = \lim_{X1 \to 0} \ln \gamma_i$, correspond to symmetrical method or normalization of the excess thermodynamic functions, namely:

$$\ln \gamma_1^0 = \Lambda_1 \neq 0, \quad \gamma_1 (X_1 \to 0) = \gamma_1^0 \neq 1, \tag{15}$$

$$\ln \gamma_2^0 = 0, \quad \gamma_2 (X_1 \to 0) = 1. \tag{16}$$

In our case, for the incomparable, it is more convenient to use the asymmetrical normalization scale (for this, one should only demand the performing of the single condition $\Lambda_1 = 0$):

$$\ln \gamma_1^0 = 0, \quad \gamma_1 (X_1 \to 0) = \gamma_1^0 = 1, \tag{17}$$

$$\ln \gamma_2^0 = 0, \quad \gamma_2 (X_1 \to 0) = 1, \tag{18}$$

$$\ln \gamma_1^{ass} \approx \sum_{i=2} i \Lambda_i X_1^{i-1}, \tag{19}$$

$$\ln \gamma_2^{ass} \approx \sum_{i=2} (1-i) \Lambda_i X_1^i. \tag{20}$$

This normalization scale will always be used by us as the default.

Let us introduce the function G^{mix}/RT (divided by RT molar Gibbs energy of mixing), the second isothermal – isobaric concentration derivative of which is equal to the full solution molar Gibbs energy:

$$G^{mix}/RT = X_1 \ln X_1 + X_2 \ln X_2 + X_1 \ln \gamma_1 + X_2 \ln \gamma_2, \tag{21}$$

$$\partial \left[G^{mix}/RT\right] / \partial X_1 =$$

$$1/X_1 + 1/X_2 - (\ln X_2 + 1) + \sum_{i=1} i^2 \Lambda_i X_1^{i-1} + \sum_{i=2} (1-i) \Lambda_i \left[i (i-1) X_1^{i-2} - (i+1) X_1^{i-1}\right], \tag{22}$$

$$\partial^2 \left[G^{mix-ass}/RT\right] / \partial X_1^2 \approx 1/X_1 + \sum_{i=2} i (i-1) \Lambda_i X_1^{i-2}. \tag{23}$$

In a completely similar manner, we can calculate (divided by RT) first isothermal – isobaric concentration derivative of the chemical potential or logarithm of the activity of the 1-st component – μ_1 and $\ln a_1$, correspondingly:

$$1/RT (\partial \mu_1 / \partial X_1) = (\partial \ln a_1 / \partial X_1) \approx 1/X_1 + \sum_{i=2} i (i-1) \Lambda_i X_1^{i-2}. \tag{24}$$

So, the equation of the diffusional (spinodal) stability loss will be the following:

$$G_{11}^{mix-ass} = \partial^2 \left[G^{mix-ass}/RT\right] / \partial X_1^2 = (\partial \ln a_1 / \partial X_1) \approx 1/X_1 + \sum_{i=2} i (i-1) \Lambda_i X_1^{i-2} = 0. \tag{25}$$

5. Application of VD-AS model to the description water soluble derivatives of light fullerenes water solutions. Calculation of nanoclusters excess functions. Miscibility gaps

Preliminary calculations show, that the 3-term approximation in the VD-AS – model (i.e. i = 2, 3, 4) is sufficient for more or less successful for the excess thermodynamic functions calculation with the satisfactory accuracy:

$$\ln \gamma_1^{ass} \approx 2\Lambda_2 X_1 + 3\Lambda_3 X_1^2 + 4\Lambda_4 X_1^3, \tag{26}$$

$$\ln \gamma_2^{ass} \approx -\Lambda_2 X_1^2 - 2\Lambda_3 X_1^3 - 3\Lambda_4 X_1^4. \tag{27}$$

So, the equation of the diffusional (spinodal) stability loss will be the following:

$$12\Lambda_4 X_1^3 + 6\Lambda_3 X_1^2 + 2\Lambda_2 X_1 + 1 = 0, \tag{28}$$

or is explicitly elementarily solved relative to X_1 (according to Cardan formula) cubic equation.

All calculated parameters for the VD-AS – model are represented in Table 2.

In all considered binary systems, we calculated the concentration dependencies $\ln \gamma_{H2O}$ (see Table 1):

$$\ln \gamma_2 = \ln \gamma_{H2O} = \ln a_{H2O} - \ln X_{H2O} = \ln a_{H2O} - \ln(1 - X_1), \tag{29}$$

and from these functions, $\ln \gamma_2(X_1)$, according to equation (27) and we determined parameters of VD-AS model: Λ_2, Λ_3, Λ_4 (see Table. 2).

TABLE 2. Parameters of model VD-AS (Λ_2, Λ_3, Λ_4) and concentration boards of diffusion instability regions ($X^{diff-instab}$) in the binary system: $C_{70}(C_6H_{13}N_2O_2)_2$ – H_2O 272.00–273.15 K

VD-AS model parameters (rel.un.)			
Λ_2 (relun.)	Λ_3 (relun.)	Λ_4 (relun.)	$\approx X^{diff-instab}$ (rel.un.)
$1.58 \cdot 10^6$	$-1.40 \cdot 10^{10}$	$4.15 \cdot 10^{13}$	$6.0 \cdot 10^{-5}$

Formally, the huge values for the summary virial coefficients Λ_i in general are not surprising, if we remember that, according to the physical sense, they are the sums of the rows, consist of probably thousands terms, responsible for the energies of interactions of a few nano-clusters with a very large number of water molecules.

Then, according to the equation (26), we calculated the concentration dependencies $\ln \gamma_1^{ass}(X_1)$(See Table 1 and Fig. 3). From Fig. 3, one can see that some dependencies $\ln \gamma_1^{ass}(X_1)$ will cross through the maximum at the values: $X_1 \approx$ *1.5·10*$^{-4}$ rel. un. (in our case it occurs slightly out of the investigated concentration range). The maximum state may be easily determined from equation (26), solving square equation:

$$1/2d\,(\ln \gamma_1^{ass}/dX_1) = \Lambda_2 + 3\Lambda_3 X_1 + 6\Lambda_4 X_1^2 = 0. \tag{30}$$

Then, according to the equation (28), we determined the boards of diffusional stability loss – X^{diff} (see Table 2 and Fig. 4), solving cubic equation:

$$F = 12\Lambda_4 X_1^3 + 6\Lambda_3 X_1^2 + 2\Lambda_2 X_1 + 1 = 0. \tag{31}$$

As one can see from Table 2, all cubic equations (28) for our considered systems have real positive roots in real concentration ranges, which correspond to the existence of liquid solutions of nano-clusters in water. From this fact, one can conclude that at some concentration range: $X_1^{diff} \approx 6.0 \cdot 10^{-5}$ rel. un. the system begins to display flaking, or perhaps pre-flaking (see later). In Fig. 4, the concentration dependencies of the diffusional instability functions $F^{diff-instab} = 12\Lambda_4 X_1^3 + 6\Lambda_3 X_1^2 + 2\Lambda_2 X_1 + 1$ are represented. From Fig. 4, we see that almost all functions $F^{diff-instab}(X_1)$ have intersections with the abscissa axis, which corresponds to diffusional stability loss.

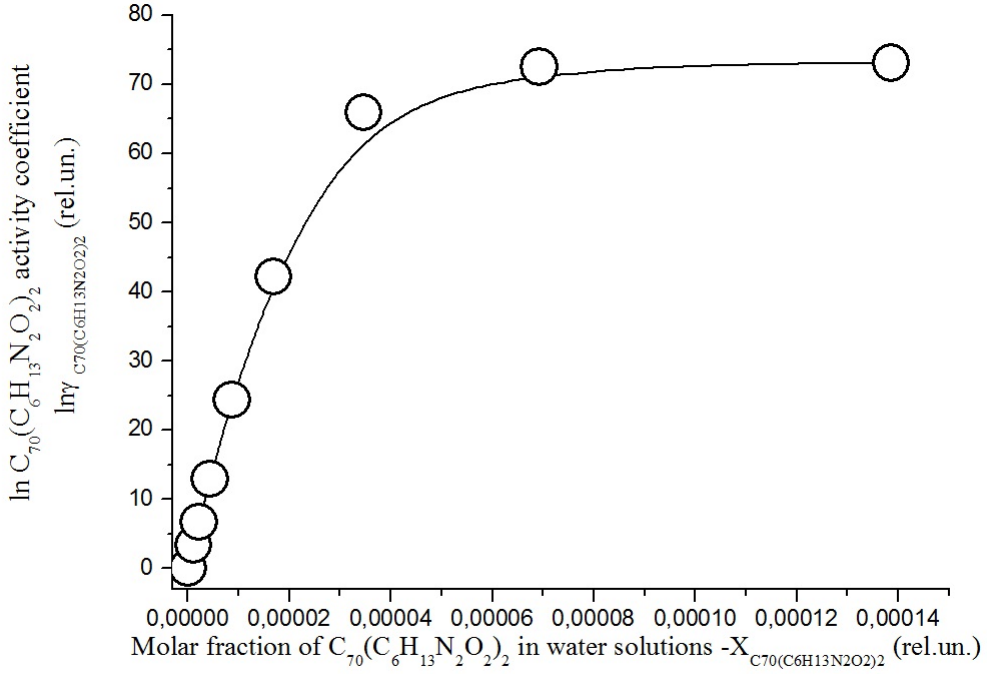

FIG. 3. Logarithm of light fullerene water soluble derivative activity coefficient ($\ln \gamma_i$) against molar fraction concentration in the binary solutions $C_{70}(C_6H_{13}N_2O_2)_2$ – H_2O at 272.99–273.15 K

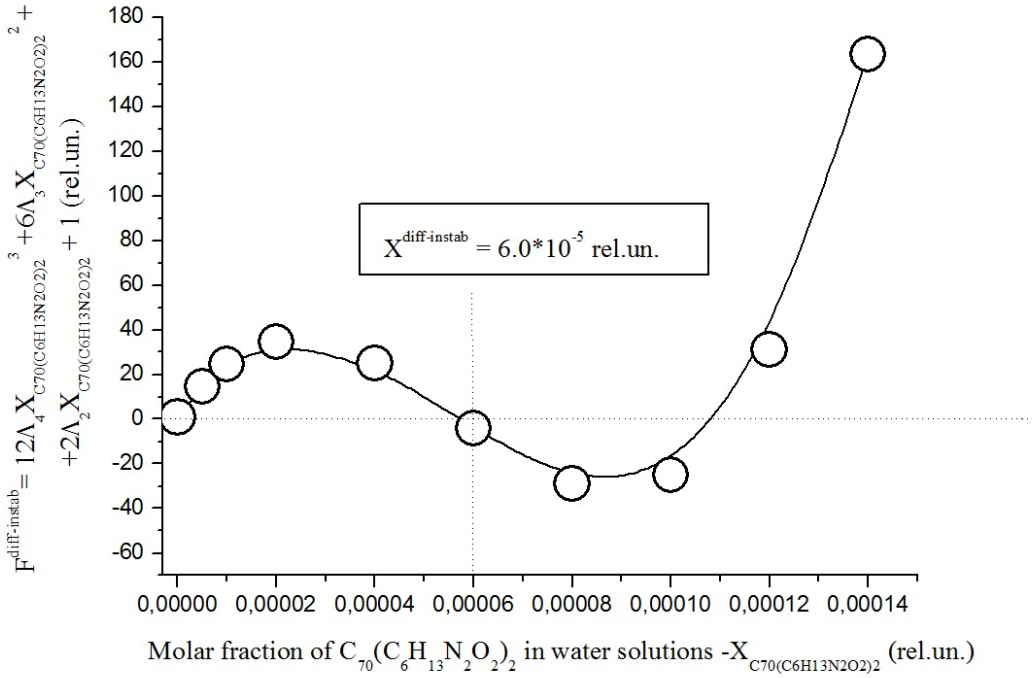

FIG. 4. Instability board function F against molar fraction concentration in the binary solutions: $C_{70}(C_6H_{13}N_2O_2)_2$ – H_2O at 272.99–273.15 K

6. Conclusions

(1) The temperature of water-ice crystallization initiation decreases in the binary water solutions of water soluble derivative of light fullerene C_{70} with the amino-acid lysine were determined at 272.99–273.15 K.
(2) Partial molar excess functions for H_2O were calculated.
(3) For the thermodynamic description of our system, we have elaborated original semi-empirical model VD-AS, based on the virial decomposition of molar Gibbs energy of the component molar fractions in the solution.
(4) With the help of VD-AS model partial molar functions of nano-clusters, excess and full average Gibbs energies for the solutions and miscibility gaps concentration regions were calculated.

Acknowledgements

Investigations were supported by Russian Found of Fundamental Investigations – RFFI (Projects NN 15-08-08438, 16-08-01206, 15-29-05837) and Fund of Assistance to Development of Small Forms of Enterprises in Scientific-Technical Sphere (Program Start 16-1, Contract No 1549C1/24357).

References

[1] Li J., Takeuchi A., Ozawa M. et al. C_{60} fullerol formation catalysed by quaternary ammonium hydroxides. *J. Chem. Soc.Chem. Commun.*, 1993, **23**, P. 1784.
[2] Chiang L.Y., Bhonsle J.B., Wang L. et al. Efficient one-flask synthesis of water-soluble fullerenes. *Tetrahedron*, 1996, **52**, P. 4963.
[3] Chiang L.Y., Upasani R.B., Swirczewski J.W. Versatile nitronium chemistry for C_{60} fullerene functionalization. *J. Am.Chem. Soc.*, 1992, **114**, P. 10154.
[4] Meier M.S., Kiegiel J. Preparation and characterization of the fullerene diols 1,2-$C_{60}(OH)_2$, 1,2-$C_{70}(OH)_2$, and 5,6-$C_{70}(OH)_2$. *Org. Lett.*, 2001, **3**, P. 1717.
[5] Szymanska L., Radecka H., Radecki J. et al. Electrochemical impedance spectroscopy for study of amyloid β-peptide interactions with (-) nicotine ditartrate and (-) cotinine. *Biosens. Bioelectron*, 2001, **16**, P. 911.
[6] Mirkov S.M., Djordjevic A.N., Andric N.L. et al. Modulating activity of fullerol $C_{60}(OH)_{22}$ on doxorubicin-induced cytotoxicity. *Nitric Oxide*, 2004, **11**, P. 201.
[7] Kokubo K., Matsubayashi K., Tategaki H. et al. Facile synthesis of highly water-soluble fullerenes more than half-covered by hydroxyl groups. *ACS Nano*, 2008, **2**(2), P. 327.
[8] Yang J.M., He W., Ping H. et al. The scavenging of reactive oxygen species and water soluble fullerene synthesis. *Chinese. J. Chem.*, 2004, **22**(9), P. 1008.
[9] Sheng W., Ping H., Jian_Min Z. et al. Novel and efficient synthesis of water-soluble [60] fullerenol by solvent-free reaction. *Synthetic Communications*, 2005, **35**(13), P. 1803.
[10] Chiang Long Y. Fullerene Derivatives as Free Radical Scavengers. US patent 5648523. July 15, 1997.
[11] Lamparth I., Hirsch A. Water-soluble malonic acid derivatives of C_{60} with a defined three-dimensional structure *J. Chem. Soc. Chem. Commun.*, 1994, P. 1727–1728.
[12] Liang Bing GAN, Chu Ping LUO. Water-soluble fullerene derivatives, synthesis and. characterization of ß-alanine C. 60 adducts. *Chinese Chemical letters*, 1994, **5**(4), P. 275–278.
[13] Kotelnikova R.A., Kotelnikov A.I., Bogdanov G.N., Romanova V.S., Kuleshova E.F., Parnes Z.N., Vol'pin M.E. Membranotropic properties of the water soluble amino acid and peptide derivatives of fullerene C_{60}. *FEBS Lett.*, 1996, **389**, P. 111–114.
[14] Hu Z., Guan W., Wang W., Huang L., Tang X., Xu H., Zhu Z., Xie X., Xing H. Synthesis of amphiphilic amino acid C_{60} derivatives and their protective effect on hydrogen peroxide-induced apoptosis in rat pheochromocytoma cells. *Carbon*, 2008, **46**, P. 99–109.
[15] Kumar A., Rao M.V., Menon S.K. Photoinduced DNA cleavage by fullerene-lysine conjugate. *Tetrahedron Lett.*, 2009, **50**, P. 6526–6530.
[16] Jiang G., Yin F., Duan J., Li G. Synthesis and properties of novel water-soluble fullerene–glycine derivatives as new materials for cancer therapy. *J. Mater. Sci: Mater. Med*, 2015, **26**, P. 1–7.
[17] Grigoriev V.V., Petrova L.N., Ivanova T.A., Kotel'nikova R.A., Bogdanov G.N., Poletayeva D.A., Faingold I.I., Mishchenko D.V., Romanova V.S., Kotel'nikov A.I., Bachurin S.O. Study of the neuroprotective action of hybrid structures based on fullerene C_{60}. *Biology Bull*, 2011, **38**, P. 125–131.
[18] Kotel'nikova R.A., Faingol'd I.I., Poletaeva D.A., Mishchenko D.V., Romanova V.S., Shtol'ko V.N., Bogdanov G.N., Rybkin A.Yu., Frog E.S., Smolina A.V., Kushch A.A., Fedorova N.E., Kotel'nikov A.I. Antioxidant properties of water-soluble amino acid derivatives of fullerenes and their role in the inhibition of herpes virus infection. *Rus. Chem. Bull.*, 2011, **6**, P. 1172–1176.
[19] Leon A., Jalbout A.F., Basiuk V.A. Fullerene-amino acid interactions. A theoretical study. *Chem. Phys. Lett*. 2008, **452**, P. 306–314.
[20] Hu Y.H., Ruckenstein E. Steam reforming products used as a hydrogen resource for hydrogen storage in Li2N. *J. Mol. Struct. Theochem.*, 2008, **865**, P. 94–97.
[21] Semenov K.N., Charykov N.A., Postnov V.N., Sharoyko V.V., Murin I.V. Phase equilibria in fullerene-containing systems as a basis for development of manufacture and application processes for nanocarbon materials. *Rus. Chem. Rev.*, 2016, **85**, P. 38–59.
[22] Semenov K.N., Charykov N.A., Murin I.V., Pukharenko Yu.V. Physico-Chemical Properties of C_{60}-tris-malonic-derivative Water Solutions. *J. of Molecular Liquids*, 2015, **202**, P. 50–58.
[23] Semenov K.N., Charykov N.A., Murin I.V., Pukharenko Yu.V. Physico-chemical properties of the fullerenol-70 water solutions. *J. of Molecular Liquids*, 2015, **202**, P. 1–8.
[24] Matuzenko M.Yu.,Shestopalova A.A., Semenov K.N., Charykov N.A., Keskinov V.A. Cryometry and excess functions of the adduct of light fullerene C_{60} and arginine –$C_{60}(C_6H_{12}NAN_4O_2)_8H_8$ aqueous solutions. *Nanosystems: Physics, Chemistry, Mathematics*, 2015, **6**(5), P. 715–725.

[25] Matuzenko M.Yu., Tyurin D.P., Manyakina O.S., Semenov K.N., Charykov N.A., Ivanova K.V., Keskinov V.A. Cryometry and excess functions of fullerenols and trismalonates of light fullerenes – $C_{60}(OH)_{22-24}$ and $C_{70}[=C(COOH)_2]_3$, aqueous solutions. *Nanosystems: Physics, Chemistry, Mathematics*, 2015, **6**(4), P. 704–714.
[26] Pitzer K.S., Pitzer K.S., *J.Phys.Chem.*, 1973, **77**(2), P. 268–277.
[27] Pitzer K.S., Kim J.J. Activity and osmotic coefficients for mixed electrolytes. *J.Amer.Chem.Soc.*, 1974, 96(18), P. 5701–5707.
[28] Filippov V.K., Charykov N.A., Rumyantsev A.V. The generalization of Pitzer's method on the system with complex formation in the solutions. Rep. Rus. Acad. Sciences. Seria: Physics-Chemistry, 1987, **296**(3), P. 665–668.
[29] Carykova M.V.,Charykov N.A. *Thermodynamic modeling of evaporate sedimentation processes*. SPb: Nauka, 2003.
[30] Charykov N.A.,Litvak A.M.,Mikhailova M.P.,Moiseev K.D., Yakovlev Yu.P. Solid solution $In_xGa_{1-x}As_ySb_zP_{1-y-z}$. New material of IR opto-electronics. I. Thermodynamic analysis of production conditions for solid solutions, iso-periodic to the substrates InAs and GaSb, by liquid phase epitaxy method. *Rus. Phys. and Tech. Semic.*, 1997, **31**(4), P. 410–415.
[31] Litvak A.M.,Charykov N.A. New thermodynamic method of calculation of melt-solid phase equilibria (for the example of A^3B^5 systems). *Rus.J.Phys.Chem.*, 1990, **64**(9), P. 2331–2335.
[32] Litvak A.M.,Moiseev K.D.,Charykov N.A.,Yakovlev Yu.P. Hetero-structures $Al_xGa_{1-x}As_ySb_{1-y}$/InAs production by LPE method. *Rus. Tech. Phys. Lett.*, 1990, **16**(13), P. 41–45.
[33] Baranov A.N., Guseinov A.A., Litvak A.M., Popov A.A., Charykov N.A., Sherstnev V.C., Yakovlev Yu.P. Production of solid solutions $In_xGa_{1-x}As_ySb_{1-y}$, iso-periodic to GaSb, nearby miscibility gap. *Rus. Tech. Phys. Lett.*, 1990, **16**(5), P. 33–38.
[34] Stringfellow G.B. Calculation of energy band gaps in quaternary III-IV alloys. *J.Elecrctron. Mat.*, 1981, **10**(5), P. 919–936.
[35] Stringfellow G.B. Calculation of ternary and quaternary III–V phase diagrams. *J.Cryst.Growth*, 1982, **58**, P. 194–202.
[36] Litvak A.M., Charykov N.A. Melt-solid phase equilibria in the system Pb-InAs-InSb. *Rus.J.Neorg.Chem.*, 1990, **35**(12), P. 3059–3062.